DETERMINING MECHANICAL PROPERTIES OF CELL MEMBRANES USING EXPOSURE-TIME CORRECTED FLUCTUATION SPECTRUM ANALYSIS

Abel Hutten

Delft,
February 4 - July 9, 2021
TU Delft
BSc program Applied Mathematics and Applied Physics

Supervisors:
Prof. Dr. Gijsje Koenderink, Department of BioNanoscience
Dr. Lisanne Rens, Department of Applied Mathematics
Lennard van Buren, PhD student, Department of BioNanoscience

Contents

Abstract

Cells and lipid vesicles have membranes with a bending modulus κ and a tension σ. Vesicle fluctuation analysis is a technique that allows one to determine these properties by examining the thermal fluctuations of the membrane. In this report we analyse and improve upon the previously implemented method of vesicle fluctuation analysis. The previous method works by extracting the spatial Fourier series of the membrane for each frame in a video of the membrane, calculating the variance of this series across all frames, and then fitting a theoretical model onto this variance on a specified mode interval. We have introduced a more objective method for determining the mode interval that should be used, and changed the model that is used in the fit to a known model that incorporates a correction for the effects of the exposure time of the camera. As a result of the changes we have implemented, we find that the results of the analysis are in better agreement with the values expected from the literature, which have been independently checked using micro pipette aspiration. The changes we have made allow an experimenter to use longer exposure times when needed, and still get accurate results.

1. Introduction

An improved understanding of the cell is the key to many invaluable technological and medical advancements, and indispensable in the pursuit of creating a synthetic cell. Creating a synthetic cell would be an immense boon to our understanding of the functioning of cells, and allow us to create technologies such as cells that produce medicines or materials, or cells that replace dysfunctional cells in the human body, for example. The cell membrane is an indispensable part of the cell, without which it could not exist. The cell membrane regulates the chemical makeup of the cell's interior, contains molecules used in a multitude of processes such as intercellular communication and chemical transport, and gives the cell its shape [1]. The mechanics of the cell membrane play a key role in fundamental cellular processes, such as cell movement and division. This makes understanding and measuring mechanical properties of cell membranes a very relevant field of study. In this report we look specifically at the bending rigidity, quantified by the bending modulus κ, and the tension σ of the membrane. Being able to measure these membrane properties allows us to do experiments on the effect on mechanical properties of using different types of lipids, or adding specific proteins to the membrane. This in turn allows us to compose a membrane that has mechanical properties that we want it to have, so that it can effectively perform the functions we want it to perform.

In order to measure mechanical properties of cell membranes or vesicle membranes constructed in the lab, multiple techniques can be used [2]. One such technique, on which we will focus our attention in this report, is the analysis of the variance of the thermal fluctuation spectrum of the cell membrane [3]. The variance of the thermal fluctuation spectrum can be obtained by filming the cell membrane as it fluctuates. Certain aspects of this process of filming the cell can introduce errors in the measured variance of the fluctuation spectrum, such as the optical resolution of the camera, length of the video and the exposure time per individual frame. In this report we will focus on the effect of the exposure time of the camera on the analysis. The currently implemented analysis does not take exposure time into account, and this likely introduces significant error in the values of the obtained mechanical properties. This research aims to better understand the problems with this implementation and to mitigate those problems by implementing a theoretical correction for the effect of exposure time. Only part of the fluctuation spectrum is relevant for this analysis. In order to determine the relevant mode regime, we implemented a different selection protocol, and the effect of this change will be explored. Another technique by which mechanical properties of membranes can be measured is micro pipette aspiration. In micro pipette aspiration, a microscopically small pipette is used to create suction on the membrane, and by inspecting the depth to which the membrane gets sucked into the pipette under a microscope, the mechanical properties can be determined. Micro pipette aspiration is not the focus of this report, but the technique was used in this report to generate a data set which we used to check the accuracy of the vesicle fluctuation analysis discussed in this report.

Some of the questions we will explore in this report deal with understanding the limitations of the previously used fluctuation analysis program. This program was developed by Francois Lienard as documented in [4], and is based on theory from [5], [6] and [7]. Our questions are: What errors do we expect to see in the values of κ and σ that are generated by the old program when the data is acquired using a non-zero exposure time? Is it possible to modify the old program to account for non-zero exposure time without changing the mode selection or theoretical model used in the fit?

Other questions deal with the changes we have made to the program. These questions are: Is the new method of mode selection more objective? Do the changes reduce the dependence of the result on camera exposure time? Do the changes reduce the systematic errors that were present in the old program? Are the results generated by the new program accurate?

We answered all of these questions by applying both programs to membranes whose properties were known from the literature, and to membranes whose properties were known from independent measurements based on aspiration and comparing, and comparing the results to the literature and to each other.

2. Theory

In this chapter we will review and discuss the theory from the literature which is relevant for this report.

2.1. The structure of a membrane, its bending modulus κ and its tension σ.

The bulk of a cell membrane is made up of phospholipids. Phospholipids are molecules with a hydrophobic tail and a hydrophilic head. Because of these properties, they arrange themselves in a tail-to-tail bilayer when placed in an aqueous solution. In addition to lipids, cell membranes also contain a large areal fraction of proteins and protein complexes, and are composed of multitude of different types of phospholipids. A schematic representation of a cell membrane is shown in figure 1.

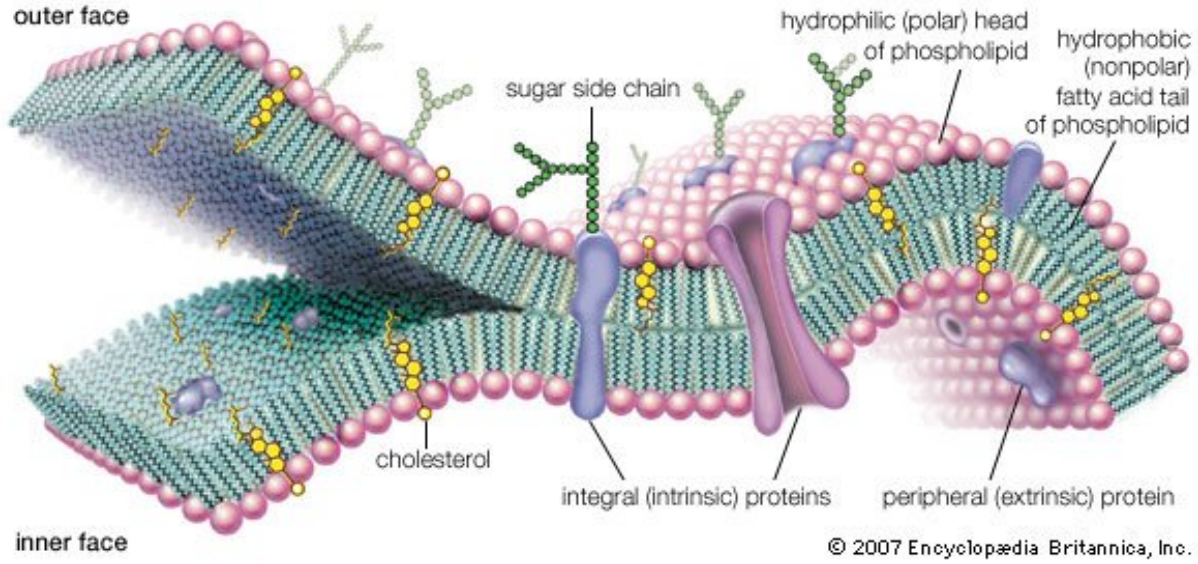

Figure 1: Schematic representation of a cell membrane. Shows inner and outer phosfolipid leaflet, integral and peripheral proteins. Some lipids and proteins on the outer face have sugar side chains. Extracted from [8].

It is currently also possible to create vesicles enclosed by a phosplipid bilayer in the lab, with techniques such as electroformation. This is done to create a simple model system of cell membranes that can be used to understand membrane mechanics, to understand protein-membrane interaction. These synthetic vesicles are also used as containers for synthetic cells.

In this report we are interested in the mechanical properties of such membranes, specifically the bending rigidity, qualified by the bending modulus, denoted κ, and the membrane tension, denoted σ.

The bending modulus of an object is defined in [9], and in the case of a membrane it quantifies the resistance the membrane has to bending. It has units of energy, and in the context of this report a natural unit for this energy is k_BT, where k_B is Boltzmann's constant and T is the temperature in degrees Kelvin. The membranes that we look at in this report are electroformed palmitoyloleoylphosphatidylcholine (POPC) membranes. POPC is a zwitterionic lipid

and the most common lipid in the plasma membrane. These membranes are known to typically have a bending modulus of between 20 - 35 k_BT [10]. The presence of dissolved sugar in the aqueous solution on the inside and outside of the membrane tends to lower this value [2]. As can be seen in [10], the bending modulus of a POPC membrane is very sensitive to experimental conditions such as temperature, formation method and the type of solution on the outside and inside of the membrane, which can cause some membranes to have outlying values within the range of 5 k_BT to 40 k_BT.

The membrane tension σ quantifies the amount of tension present in the membrane, in units of N/m. Such tension can be caused by factors such as an osmotic pressure difference between the inside and outside of the membrane. In this report we consider only the possibility for positive values of σ, and we constrain our analysis accordingly. For the membranes we examine in this report the tension tends to be low, in the order of $10^{-8}N/m$, and the mechanics tend to be dominated by the bending rigidity [2].

2.2. Adimensional membrane fluctuation spectrum

Since the vesicles studied in this report have a radius in the order of tens of μm and are flexible with bending moduli in the order of tens of k_BT. The membranes fluctuate visibly when looked at under an optical microscope, as a result of random thermal fluctuations. The exact way in which a membrane's shape fluctuates is uniquely dependent on the membrane's bending modulus κ and tension σ [11]. Therefore the values of κ and σ can in theory be uniquely determined when the way in which the membrane fluctuates is known.

In fact, it is sufficient to know the way the membrane's shape fluctuates in the equatorial plane in order to determine κ and σ [11]. In the equatorial plane, the membrane's position is a one-dimensional contour, as illustrated in figure 2.

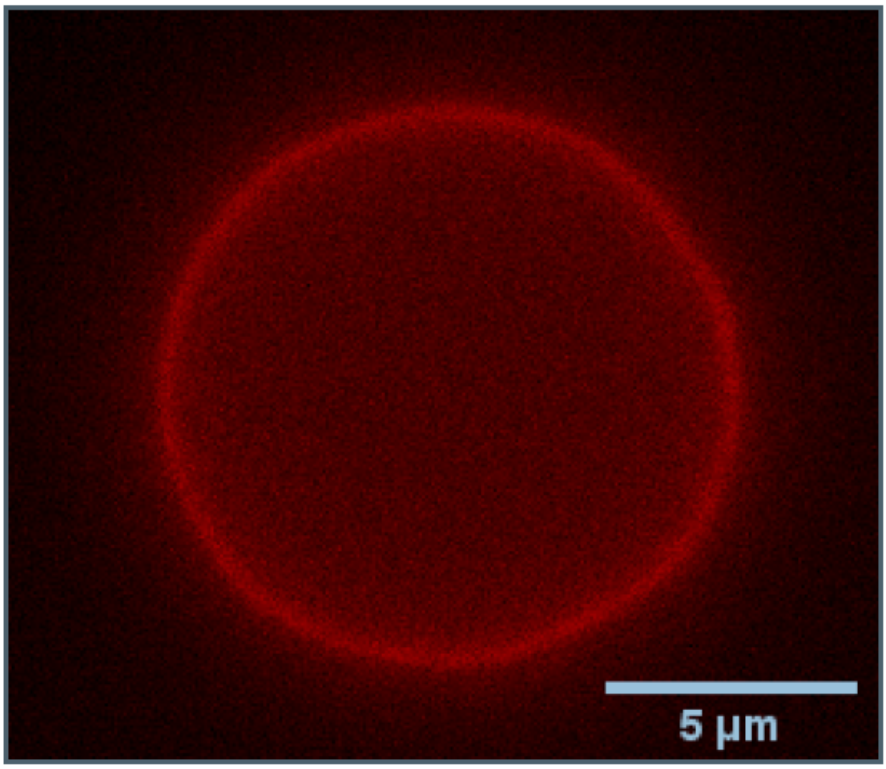

Figure 2: The contour of a membrane in the equatorial plane. Picture extracted from [4].

This contour can be described in polar coordinates as $r(\theta)$, the distance of the membrane from its center when measured at an angle θ relative to some fixed diameter line. $r(\theta)$ can be developed in Fourier modes [11],

$$r(\theta) = R\left(1 + \sum_{n=1}^{\infty} a_n cos(n\theta) + b_n sin(n\theta)\right) \tag{1}$$

where R is the vesicle radius. Each mode number n has an associated wave number l, such that $l = \frac{n}{R}$ [11]. The modulus $|c_n|$ is defined as $|\sqrt{a_n^2 + b_n^2}|$, and all the information necessary to determine κ and σ is contained in the variance of $|c_n|$ over time, that is var$(|c_n|) = \langle|c_n|^2\rangle - \langle|c_n|\rangle^2$, where $\langle\cdot\rangle$ denotes the average taken over time. Var$(|c_n|)$ is called the adimensional fluctuation spectrum of the membrane [11], but will often be referred to as simply the fluctuation spectrum of the membrane throughout this report. Var$(|c_n|)$ is known theoretically as a function of κ and σ in the case of spherical and planar membranes [11].

The adimensional fluctuation spectrum of a spherical membrane in the equatorial plane, as a function of κ and σ, is given as

$$var(|c_p|) = \frac{1}{4} \cdot \sum_{n=p}^{n=n_{max}} \frac{2n+1}{\pi} \frac{(n-p)!}{(n+p)!} \left(P_n^p(0)\right)^2 \frac{k_B T}{\kappa \lambda_n} \tag{2}$$

where $var(|c_p|)$ is the value of the adimensional fluctuation spectrum at mode p, n_{max} is the cut-off of the shortest possible wavelength. $P_n^p(x)$ is the associated Legendre Polynomial as defined in reference [12], and where

$$\lambda_n = n^2(n+1)^2 - (2-\bar{\sigma})n(n+1)\ ,\ \bar{\sigma} = \frac{\sigma\langle R\rangle^2}{\kappa}.$$

n_{max} is estimated to be around 10^4, but converges rapidly for low to moderate tension, making it sufficient to consider only a few hundred terms [6]. Eq. 2 has been derived by assuming the energy of the vesicle is given by the Helfrich equation [13], and by assuming that the excess area, defined as the area of the membrane minus the area of a sphere of the same volume as the vesicle, is constant. It has further been assumed that the fluctuations take place in the low Reynolds number limit. In that limit, both the inertial and convective terms of the Navier-Stokes equation [14] can be neglected. Assuming the fluid in and around the vesicle is incompressible and satisfies the no-slip condition at the contact surfaces with the membrane, the Navier-Stokes equations give the flow fields of the fluid in and around the membrane. From the normal component of this flow field, the rate of change of the membrane position is calculated, and from that rate of change Eq. 2 follows [15]. All of the assumptions that were made in this derivation hold to a sufficient degree for the membranes we look at in this report [6].

The adimensional fluctuation spectrum of a straight line contour in a planar membrane is given as

$$var(|c_n|) = \frac{1}{4}\cdot\frac{k_BT}{\pi\langle R\rangle^3\sigma}\left[\frac{\langle R\rangle}{n} - \frac{1}{\sqrt{\frac{\sigma}{\kappa}+\frac{n^2}{\langle R\rangle^2}}}\right] \tag{3}$$

Eq. 3 is useful since, as stated in [11], for $n \geq 5$ the difference between Eq.2 and 3 becomes negligible when we assume that the vesicle is quasi-spherical and that the spontaneous curvature is negligible.

Equations 2 and 3 for var(c_n) are modified versions of those found in [11]. The modification we have made is the factor $\frac{1}{4}$ present in both these formulas. A justification for this modification is presented in section 4.1.

2.3. Fluctuation lifetime and the effect using a camera to obtain the adimensional fluctuation spectrum

When a spherical membrane deformation is caused by thermal interactions of the membrane with its environment, this causes specific Fourier mode amplitudes $|c_n|$ to increase. These modes then vibrate as standing waves. These standing waves get damped over time due to viscous drag from the surrounding fluid, thereby lowering $|c_n|$ over time. The rate at which these waves are damped is characterised by the fluctuation lifetime τ_m(n), which is given as follows [11]:

$$\tau_m(n) = \frac{4\eta\frac{n}{\langle R\rangle}}{\sigma\left(\frac{n}{\langle R\rangle}\right)^2 + \kappa\left(\frac{n}{\langle R\rangle}\right)^4} \tag{4}$$

where η is the viscosity of the medium.

In practice, var($|c_n|$) can be obtained by making a video of the membrane, calculating the Fourier spectrum for each frame, and then taking the variance of this spectrum over all frames. In order for this sampled adimensional fluctuation spectrum to accurately resemble the actual adimensional fluctuation spectrum, the video must be taken over a long enough period

that the sampled adimensional fluctuation spectrum converges to the actual adimensional fluctuation spectrum. When the sample length is multiple times the fluctuation lifetime for a mode, it can be assumed that the sampled adimensional fluctuation spectrum accurately resembles the true value for that mode. Therefore, the length of the video determines for which modes the adimensional fluctuation spectrum can be retrieved accurately. For modes with low mode numbers, and therefore high fluctuation lifetimes, the adimensional fluctuation spectrum is not useful and should be discarded from the analysis. At high mode number on the other hand, the spatial frequency of the modes becomes higher than the spatial resolution of the camera. These modes can therefore not be observed accurately and the adimensional fluctuation spectrum at these modes is not useful and should be excluded from the analysis.

Although its not immediately obvious from the formulas, in [6] it is stated that var($|c_n|$)$\cdot n^3$ is independent of n for intermediate modes. One can therefore plot var($|c_n|$)$\cdot n^3$ and discard any modes for which this value is not constant in order to exclude those modes which are significantly affected by the poor statistics or insufficient camera resolution [11].

Finally, at higher mode numbers another factor needs to be kept in mind: the exposure time that the camera needs for each frame, denoted τ or T, causes a lowered time resolution. Therefore, Fourier modes for which the amplitude of $|c_n|$ changes significantly during the exposure time of a single frame will not be imaged accurately. This mainly affects those modes for which the fluctuation lifetime is equal to or smaller than the exposure time. This results in a critical mode n^C, which is the highest mode for which the exposure time is lower than the fluctuation lifetime [11]. Assuming the mechanics of the membrane are mainly determined by the bending modulus, as is the case for the membranes which we look at in this report, the critical mode depends only on κ and τ, and is given explicitly by Eq. 5 [11].

$$n^C = \sqrt[3]{\frac{4\eta}{\kappa\tau}} \tag{5}$$

where η is again the viscosity of the medium. Table 1 shows values of n^C for typical κ, σ and τ.

Table 1: Typical critical mode n^C, as a function of exposure time. These values assume a κ of $30\ k_BT$ and a σ of 10^{-8} N/m.

Exposure time τ (ms)	Typical n^C
2.5	27
5	21
10	17

For the modes that can still be imaged with sufficient accuracy despite the exposure time, the smudging caused by the exposure time still affects the adimensional fluctuation spectrum [11], but it does so in a predictable manner. The adimensional fluctuation spectrum we expect to see when the vesicle is measured with an exposure time τ is given in Eq. 6, and is a modified version of the formula given in [11] that includes the factor $\frac{1}{4}$ The justification for the modification can be found in section 4.1. ζ is defined to be equal to $\frac{n_x}{n_y}$, where n_x is the Fourier mode number of the membrane in the plane of the observed contour, denoted as in this report as n, and n_y is its mode number in a contour perpendicular to the observed contour. The exposure time corrected fluctuation spectrum is given as an integral over all wave numbers in the perpendicular direction, which is equivalent to an integral over ζ.

$$var(|c_n|) = \frac{1}{4} \cdot \frac{2}{\pi^2 \langle R \rangle^3} \int_0^\infty \frac{k_B T \tau_m^3}{\tau^2} \frac{1}{4\eta \frac{n}{\langle R \rangle} \sqrt{1+\zeta^2}} \cdot \left(\frac{\tau}{\tau_m} + exp\left(-\frac{\tau}{\tau_m} \right) - 1 \right) \frac{n}{\langle R \rangle} \, d\zeta \quad (6)$$

where

$$\tau_m = \frac{4\eta \frac{n}{\langle R \rangle} \sqrt{1+\zeta^2}}{\sigma \frac{n^2}{\langle R \rangle^2} (1+\zeta^2) + \kappa \frac{n^4}{\langle R \rangle^4} (1+\zeta^2)^2}$$

is the formula for the fluctuation lifetime in the ζ coordinate system. This formula is derived by assuming the equation for the position of the fluctuating membrane is given by the Langevin equation [16], and that the viscous relaxation term in this equation is dominant, so that the permeation term can be neglected. From this equation with the permeation term neglected, the auto-correlation function is then calculated and integrated over one integration time, resulting in Eq. 6.

3. Computational Procedure

In this section, we describe the methods used to answer each of the research questions posed in the introduction. We will also briefly go over the old method of analysis and we will explain what changes we have implemented to that method.

3.1. The old method of analysis

For a detailed explanation of the old method of analysis, consult [4]. Its main structure will be explained in this section.

The goal of the analysis is to obtain values of the bending modulus κ and tension σ of a membrane from a video of that membrane. Two frames of such a video, chosen one second apart, are shown in figure 3.

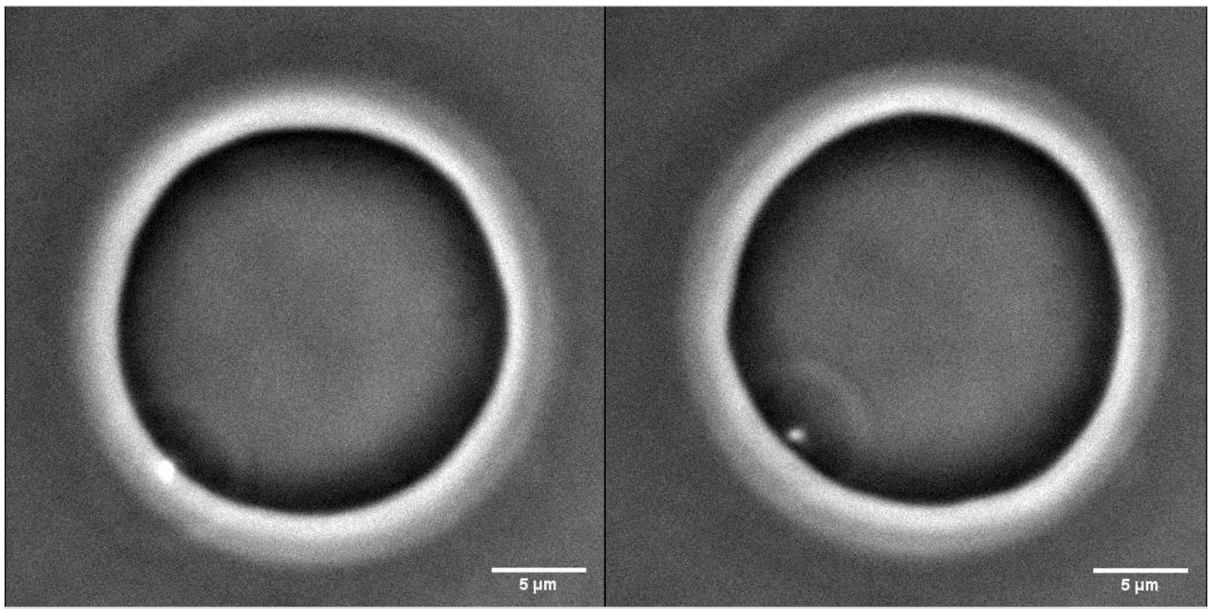

Figure 3: Two frames taken from a video of a fluctuating membrane, 1 second apart.

The first step is to determine the position of the membrane in each frame of the video. This is done by drawing radial lines through the center of the vesicle, and selecting the points on those lines where the brightness changes most rapidly. Next this membrane position is expressed in polar coordinates as $r(\theta)$, and the average radius $\langle R \rangle$ is calculated. Then $r(\theta)$ is expressed as a Fourier series, and the modulus $|c_n|$ of each Fourier mode n is calculated for each frame. Finally, the variance of $|c_n|$ is calculated across all frames. This is the observed adimensional fluctuation spectrum, and it will be used to find κ and σ by fitting a model for the theoretical adimensional fluctuation spectrum that depends on κ and σ to it. This part of the analysis has not been changed, and is therefore not the focus of this report. Not every mode should be used for the fit, as explained in chapter 2. The old method of mode selection works by creating a plot of var($|c_n|$)$\cdot n^3$, and selecting the modes for which this plot is constant as the fit interval. This plateau selection is done by the experimenter through visual inspection of the plot. An example of a typical var($|c_n|$)$\cdot n^3$ plot is shown in figure 4, together with an indication of the plateau interval.

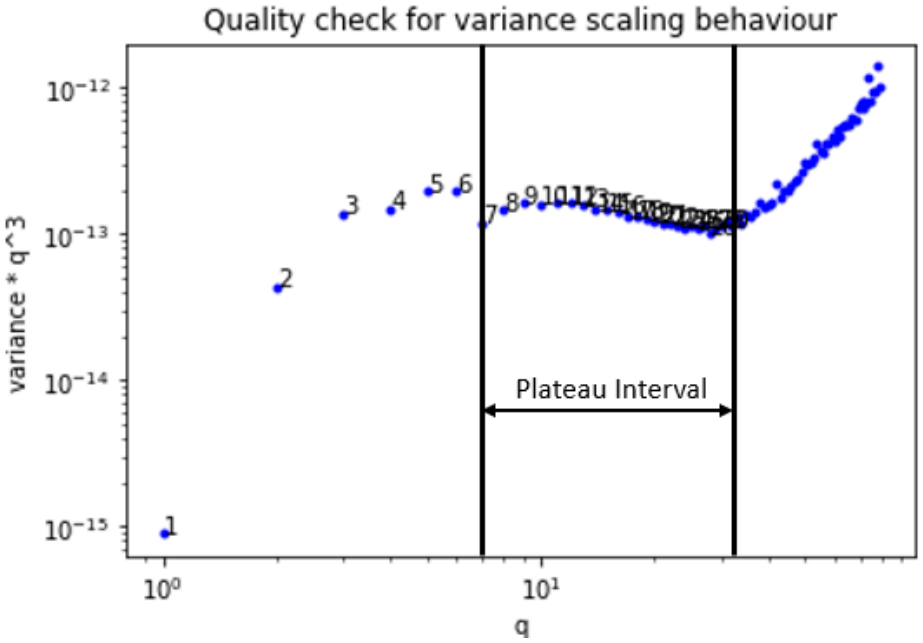

Figure 4: Plot of var($|c_q|$)·q^3 as a function of the mode number q, together with an indication of the plateau interval. Data from a GUV made of POPC, filmed with an exposure time of 5 ms. The vesicle was prepared and filmed by Lennard van Buren, and the details of this process can be found in section 3.6.

Once the fit interval has been determined,a fit is performed. The fit is a nonlinear least squares fit, which takes a model that depends on any number of parameters, and a domain together with a target data set on that domain. It also takes constraints that the parameters need to satisfy. It then uses the Trust Region Reflective algorithm to find the values of the parameters that minimize the sum of the squared residuals. The Trust Region Reflective algorithm is generally robust [17]. We supply this fitting algorithm with Eq. 2 as its model, which depends on the parameters κ and σ. κ and σ are constrained to be positive. The domain over which the fit is performed is that over which the plot of var($|c_n|$)·n^3 was determined to be constant in the previous step. The data set to which the model is fit is the adimensional fluctuation spectrum that has been determined from the video. κ and σ result from this fit.

3.2. Examining the effects of fitting a model for the fluctuation spectrum at zero exposure time to data obtained with non-zero exposure time

The old method fits a theoretical model for the adimensional fluctuation spectrum that assumes zero exposure time, Eq. 2, to an observed adimensional fluctuation spectrum that was obtained using a camera with non-zero exposure time. In order to get an idea of the effect this has on the value of κ and σ resulting from the fit, we want to compare the theoretical effect of changing the exposure time at constant σ and κ, i.e. changing τ in Eq. 6 while keeping σ and κ constant, to the theoretical effect of changing κ and σ at zero exposure time, i.e. changing either κ or σ in Eq. 2. We do this by making three plots of var($|c_n|$) versus n, with the same baseline values for κ and σ, each showing the effect of changing one of the relevant parameters. The baseline values of κ and σ we choose are values typical for the membranes studied in this report, namely 30 k_BT and 10^{-8} N/m respectively, as was the displayed mode interval, which was [10,40]. The

plot for different exposure times is made using Eq. 6, while the other two plots are made with Eq. 2, one with varying κ and the other with varying σ. Examining these plots will allow us to determine the effects of fitting a model for the fluctuation spectrum at zero exposure time to data obtained with non-zero exposure time.

3.3. Examining the need for an exposure time dependent model for the fit procedure

We wish to know if it is possible to find the bending rigidity and tension of a membrane which has been filmed at non-zero exposure time by first modifying the observed spectrum in a way that reverses the effect of the exposure time, and then fitting the model for the zero exposure time spectrum to this modified spectrum, since that would allow us to correct for the exposure time without altering the mode selection or the fit model. The only way this would be possible is if the effect of the exposure time on the observed spectrum is known beforehand, and the effect of filming with non-zero exposure time is to transforms the observed spectrum injectively (i.e. if any two membranes give a different fluctuation spectrum when filmed with zero exposure time, they must again give different spectra when filmed with non-zero exposure time). Our goal is to find σ and κ, which are not known beforehand, so we need to check whether the effect of non-zero exposure time depends on κ and σ. We check this by plotting the ratio of the theoretical 30 ms exposure time spectrum, Eq. 6 with τ = 30 ms, to that of the theoretical zero exposure time spectrum, Eq. 2, for different values of κ and σ. Both κ and σ are chosen in the range typical for the membranes on which we focus in this report, and τ = 30 ms is picked arbitrarily since we just need a single counterexample. If this ratio is dependent on the choice of κ and σ, we know that we need an exposure time dependent model in the fit procedure. As shown in figure 6 in the results, the ratio did depend on both κ and σ.

3.4. The new method of mode selection

As stated, the old method of mode selection works by creating a plot of var($|c_n|$)$\cdot n^3$, and selecting the modes for which this plot is constant as the fit interval. An example of a typical var($|c_n|$)$\cdot n^3$ plot is shown in figure 4. As is clear from this figure, it is not objectively obvious at which mode interval the value of var($|c_n|$)$\cdot n^3$ is constant; one experimenter might say it starts at mode 3 and ends at mode 40, while another might say it starts at mode 10 and ends at mode 30, for example, and such different choices produce values for κ that are significantly different from one another; the first experimenter would get a κ of 30.2 k_BT, while the second would find κ = 38.5 k_BT for this data set.

We attempted to reduce the dependence of the result on subjective choices by implementing a different process of mode selection. Our new method, which is a combination of the methods described in [6] and [11], also attempts to take into account that the modes with smaller fluctuation lifetime have not been imaged correctly, and should be excluded from the fit procedure. We will first determine the upper limit of the fit interval, and then use a method from [6] to determine κ. This then allows us to find σ. Our method starts by using Eq. 5 with a guess for κ to find the highest mode we allow for the fit. We do not need to take the spatial resolution of the camera into account, since that starts to negatively effect the quality of the spectrum at much higher modes than the temporal resolution, which effects the quality relatively sooner, for exposure times and camera resolutions looked at in this paper [11]. The guess for κ does

not need to be perfect, since Eq. 5 is only weakly dependent on κ in the typical range, and the final values of the analysis are also only weakly dependent on the choice of upper mode. If the analysis results in a κ that differs from the guess by a significant amount, the experimenter can use this resulting κ as the guess instead and run the analysis again, repeating this process until the resulting κ is similar enough to the guessed κ. In practice this recursive process is almost never necessary.

Once we have the upper mode of the fit range, we use the method described in [6] to deal with the lowest mode. This method works as follows. The fit is run for each possible choice of initial mode and the determined upper mode, and both κ and σ are allowed to take any positive value. The κ value resulting from each fit is plotted against the initial mode, to produce a plot of κ as a function of the initial mode. A typical example of such a plot is shown in figure 5, made with the same data set as figure 4.

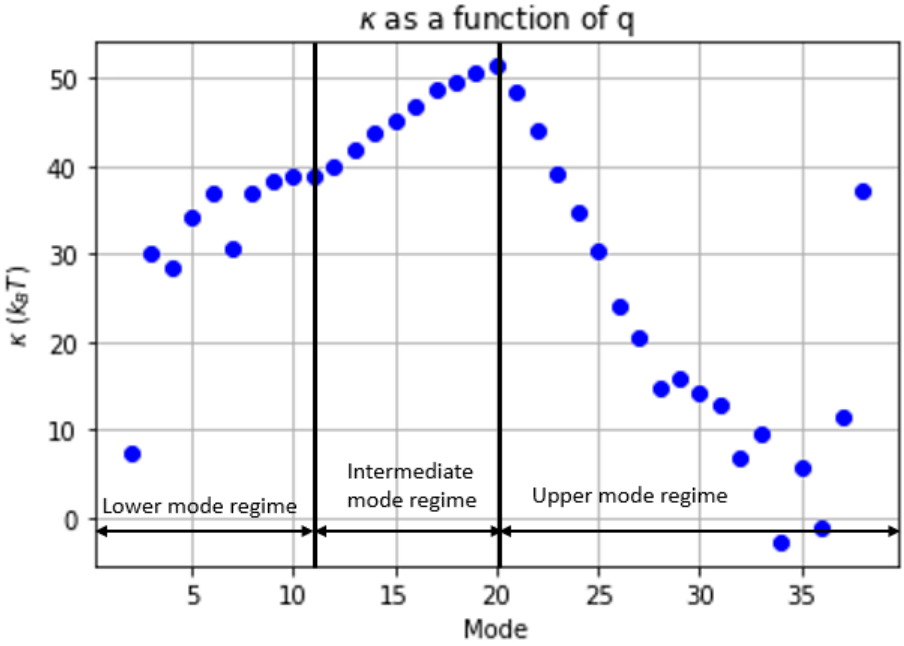

Figure 5: κ as a function of the initial mode in the fit range, for the same data set as figure 4. This is data from a GUV made of POPC, filmed with an exposure time of 5 ms. The vesicle was prepared and filmed by Lennard van Buren. The approximate locations of the three mode regimes have been indicated.

This plot contains three regimes; the lower mode regime, the upper mode regime and the intermediate mode regime. The regime of interest is the intermediate regime, as explained in [6]. The intermediate mode regime is located where the graph is relatively least dependent on the mode, and it is followed by the upper regime which typically has a downwards slope. In figure 5 we can clearly identify the end of the intermediate regime at mode 20, but the beginning is not so clear. It is typical for the end of the intermediate mode regime to be more clear while the beginning is more ambiguous. Some experimenters might choose it at mode 9 while others could choose it at mode 16. As explained in the section on Results and Discussion, the subjectivity in the choice of intermediate regime has only a limited impact on the final result of the analysis.

Once the experimenter has selected the intermediate regime, κ is taken to be the average

value of all κ values in this regime. σ is then fitted using this value of κ, the upper mode as found before and the average mode of the intermediate regime as its initial mode. The average mode is chosen to make the values of κ and σ as consistent as possible.

3.5. The new fit model

In order to account for the effect of exposure time on the adimensional fluctuation spectrum, we use Eq. 6 for the fit of the adimensional fluctuation spectrum instead of Eq. 2, since Eq. 6 takes exposure time into account.

3.6. Determining whether the implemented changes have reduced the dependence of the result on the exposure time and improved the result

In order to check whether the changes we have made to the analysis have indeed reduced the dependence of the result on the exposure time that was used to take the measurement, and to see whether the accuracy of the result has improved, we take measurements of vesicles for which the correct value of κ is approximately known from the literature ([10]) at multiple different exposure times. We then analyse the results on the extent to which the average values of the obtained κ's depend on the used exposure time, and the spread in the values generated by the different methods. We do this for the old method, the old method with the new mode selection, and the new method that has both the new mode selection and the new model for the adimensional fluctuation spectrum, in order to analyse the effect of each implemented change individually. We also calculate and plot the σ's for all these measurements in order to examine the impact the changes have on the value the program generates for σ.

For completeness, a description of the vesicle preparation process will now be given. Vesicle preparation and video capture was done by Lennard van Buren, and the following description of these processes has been supplied by him, reproduced here unedited.

Vesicle formation, written by Lennard van Buren:

DOPC membranes for exposure time measurements were made by electroformation [18].

In short, 5 microL of lipids at 1 mg/mL were spread over two platina electrodes. Lipids were dried for 30 minutes in a vacuum desiccator. Then, an electroformation chamber was filled with swelling buffer containing 200 mOsm sucrose and 10 mM Tris-HCl pH 7.4. After inserting the electrodes, vesicles were formed by electroformation for 90 minutes at 300 Hz and 2 V_{pp} using a function generator. After formation, vesicles were detached from the electrodes by firmly tapping the electroformation chamber on a table.

POPC and POPC with cholesterol membranes were made by gel-swelling [19]. 24x24 mm coverslips were first rinsed with water and ethanol and then plasma cleaned for 30 seconds. Then, 100 microL of a 5% (w/v) PVA solution in 200 mOsm sucrose was added to the coverslip. The excess fluid was taken off with a tissue. The gel was then baked for 30 minutes at 50 degrees. After that, 10 microL of 1 mg/mL lipid solution was spread over the gel and dried for 30 minutes under vacuum. Swelling was initiated by adding 300 microL of a 200 mOsm sucrose buffer containing 10 mM Tris pH 7.4 to the gel. After swelling for 1 hour, vesicles were harvested by collecting the solution from the coverslip and flushing it once again over the

coverslip.

Vesicle fluctuation analysis video capture process, written by Lennard van Buren:

After vesicle formation, 5 microL of vesicles was added to an observation chamber containing 15 microL of 200 mOsm glucose and 10 mM Tris pH 7.4. The observation chamber was passivated with a 1 mg/mL beta-casein solution prior to prevent membrane adhesion to the glass surface. For fluctuation recordings, vesicles were picked with radius larger than 5 micron, with membranes that were clearly fluctuating and did not show secondary structures. Furthermore, we only recorded vesicles that were clearly isolated from other vesicles or dirt. Membranes were recorded in the equatorial plane. For each fluctuation recording, 2000 images were continuously acquired with an exposure time varying from 1 to 5 ms.

All membranes contained 0.1% (mol/mol) ATTO 655 DOPE for fluorescent imaging.

3.7. Comparing the improved fluctuation analysis to an independent measurement

Although a rough estimate is known for the values of κ of the vesicles used in the experiment that is described in the previous subsection, we also want to have a more accurate way to check whether our improved fluctuation analysis produces correct results for κ. We test this by creating a single batch of vesicles, taking two random samples from this batch, analysing one batch with micro pipette aspiration and the other with fluctuation analysis, and then comparing the results.

For completeness, a description of the micro pipette aspiration process has been added. The micro pipette aspiration measurements were performed by Lennard van Buren, and the description of this process has been supplied by him, reproduced here unedited.

Micro pipette aspiration, written by Lennard van Buren:

To probe membrane bending rigidity in an independent manner, we performed micropipette aspiration experiments. We used an aspiration chamber that was closed from the top and bottom. A glass pipette was pulled and forged to an opening of about 5 – 8 micron. The pipette was inserted in the chamber, and both pipette and chamber were passivated with a 5 mg/mL beta-casein solution for 30 minutes. Then, the beta casein solution was removed and the chamber was washed twice with observation buffer (200 mOsm glucose + 10 mM Tris pH 7.4), after which the chamber was left filled with 100 microL observation buffer. Then, 10 microL of vesicles were added. The sample was left open for 5 – 15 minutes until vesicles were clearly fluctuating. After that, the chamber was closed with mineral oil to prevent further evaporation.

For aspiration, a fluctuating vesicle was selected without secondary structures. To grab the vesicle, aspiration pressure in the pipette was slightly increased by lowering a water bath that was connected to the pipette via tubing filled with water. The vesicle was then prestressed by increasing aspiration pressure to 100 mm and keeping it there for 2-3 minutes. After that, aspiration pressure was decreased back to 0.1 mm. To record the bending deformation, the aspiration pressure was stepwise increased from 0.1 to 30 mm in 50 steps. After every step, the stage was held stable for 2 seconds, and then a fluorescent image was taken. After each aspiration experiment, the vesicle could be released by bringing the aspiration pressure back to

0.

Aspiration data was analysed by Lennard van Buren following [20].

Image analysis yielded the membrane area in each image as well as the membrane tension. Finally, bending rigidities were fitted to the low tension regime (lower than 0.5 mN/m) of the area dilation curve.

4. Results and Discussion

In this chapter the obtained results will be presented and discussed.

4.1. Examining the effects of fitting a model for the fluctuation spectrum at zero exposure time to data obtained with non-zero exposure time

In order to get an idea of the type of error we would expect to see in the values of κ and σ when using the formula for the zero exposure time spectrum in the analysis of a data set obtained with non-zero exposure time, we want to compare the theoretical effect of changing the exposure time at constant σ and κ to the theoretical effect of changing κ and σ at zero exposure time. This was done by making three plots of var($|c_n|$) versus n, with the same baseline values for κ and σ, each showing the effect of changing one of the relevant parameters. The baseline values of κ and σ were values typical for the membranes studied in this report, as was the displayed mode range. The plot for different exposure times is made using Eq. 6, while the other two plots are made with Eq. 2. The resulting plots are shown in figure 6.

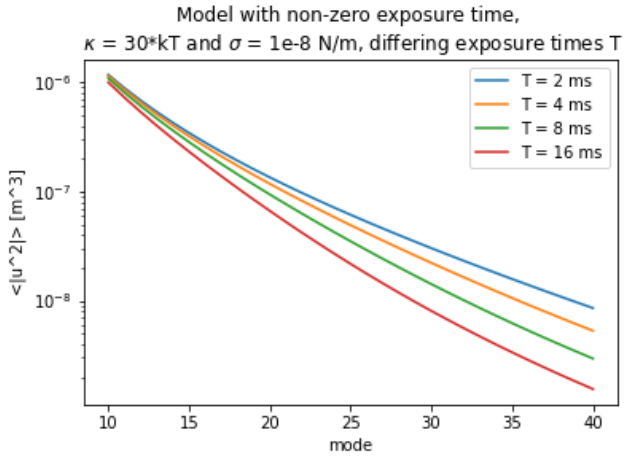

(a) Effect of increasing exposure time T

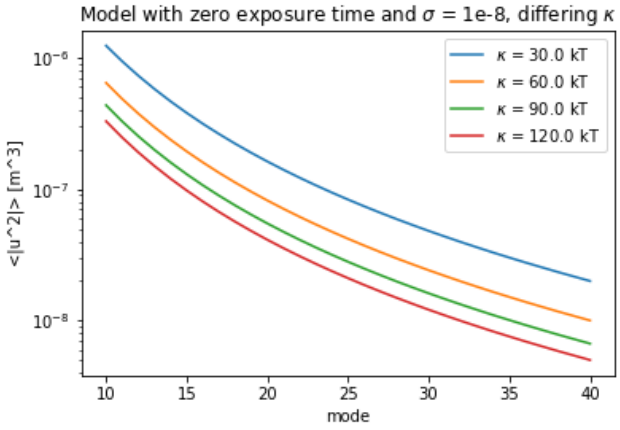

(b) Effect of increasing κ

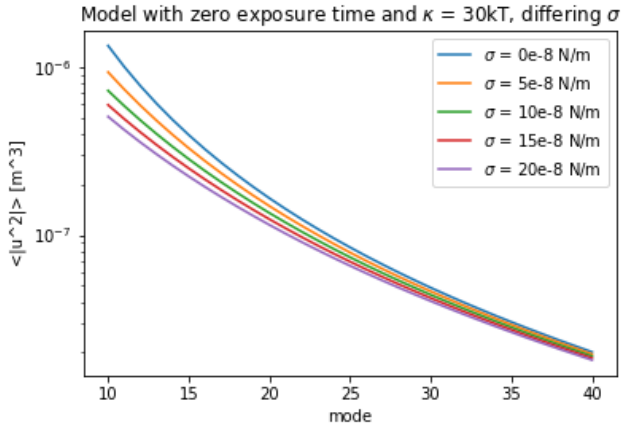

(c) Effect of increasing σ

Figure 6: A comparison of the theoretical effect of increasing the exposure time at fixed κ and σ (panel a), the theoretical effect of increasing κ at zero exposure time (panel b), and the theoretical effect of increasing σ at zero exposure time (panel c). Figures are made with values of κ and σ typical for the vesicles studied in this report, and displayed over the mode range that is most relevant for this report.

From figure 6a we see that increasing the exposure time is predicted to lower the values of the observed adimensional fluctuation spectrum, and more so with higher modes than with lower modes. The effect of increasing κ for a spectrum obtained with zero exposure time is to lower the entire spectrum in a manner that is near uniform in the relevant mode number range (figure 6b). Increasing σ also lowers the value of the spectrum, but does this more at the lower modes than at the higher modes (figure 6c). Therefore it is reasonable to expect that when we fit the model with zero exposure time to a spectrum obtained with finite exposure time, this will give a value of κ that is too high. This is because the exposure time lowers the value of the observed spectrum at the higher modes, and a higher value of κ will lower the fit spectrum in that mode range too and thus minimize the discrepancy between the two. The higher κ causes the fit spectrum to be lowered at the lower modes too (figure 6b), but increasing the exposure time does not lower the spectrum to decrease significantly at those modes (figure 6a). This causes a discrepancy at the lower modes, but because this discrepancy exists at only a small

range, the mean squared error will still be made smaller by fitting κ that is higher than the true κ, and therefore the fit will still produce an overestimate of κ. In order to compensate for the discrepancy at the lower modes, the program will then give a σ that is lower than the true σ, since that raises the value of the fit spectrum at the lower modes and counters the effect of a κ that is too high. We therefore expect a that when we fit the model with zero exposure time to a spectrum obtained with non-zero exposure time, we will obtain a κ that is too high and a σ that is too low. In the following subsections we do indeed see evidence that this is happening in the old method of analysis.

4.2. Substantiation of the need for an exposure time dependent model for the fit procedure

As stated, we wish to know if it is possible to find the bending rigidity and tension of a membrane which has been filmed at non-zero exposure time by first modifying the observed spectrum in a way that reverses the effect of the exposure time, and then fitting the model for the zero exposure time spectrum to this modified spectrum. As stated, we have chosen to do this by plotting the ratio of the theoretical 30 ms exposure time spectrum, Eq. 6 with τ = 30 ms, to that of the theoretical zero exposure time spectrum, Eq. 2, for different values of κ and σ. The resulting plot is shown in 7.

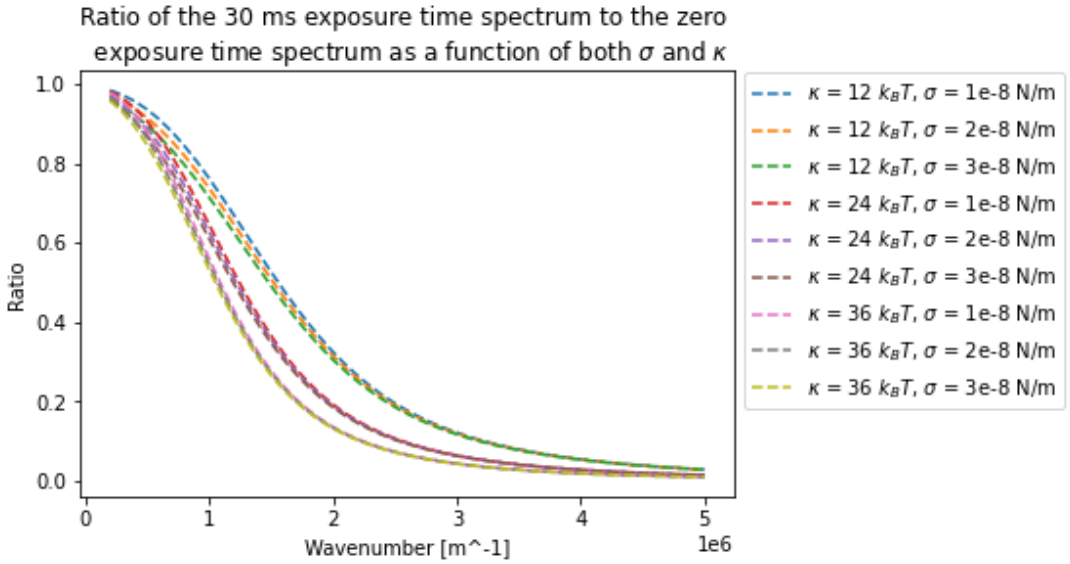

Figure 7: The ratio of the theoretical 30 ms exposure time spectrum to the theoretical zero exposure time spectrum for different combinations of σ and κ.

From this plot we see that at an exposure time of 30 ms we do indeed have a dependence of the ratio on both κ and σ. This example implies that it is in general impossible to find the bending rigidity and tension of a membrane which has been filmed at non-zero exposure time by first modifying the observed spectrum in a way that reverses the effect of the exposure time, and then fitting the model for the zero exposure time spectrum to this modified spectrum. This is to be expected since the relaxation time of a vibrational mode, Eq. 4, depends on both

σ and κ, and the relationship between the fluctuation lifetime and the exposure time is what determines the magnitude of the effect of the exposure time on the observed variation in mode amplitude. We therefore can not use Eq. 2 in our fit procedure and must use Eq. 6 instead.

4.3. Justification for the added factor $\frac{1}{4}$ in the formulas for the adimensional fluctuation spectrum of a fluctuating vesicle.

As stated, we have implemented a modified version of the formulas for the adimensional fluctuation spectrum found in [11]. We have modified these formulas by adding the prefactor of $\frac{1}{4}$ because we believe that its absence in that paper is erroneous [21]. In this subsection we present a justification for this claim.

The best way to show that the prefactor should be present in the formulas would be to work through the derivation of those formulas. Due to time constraints, it was not possible to derive the formula within this project. Instead, we justify our claim by showing the discrepancies between different models in absence of the correction factor. Both [11] and [6] contain a formula for the mean square amplitude of the spherical harmonic modes of a quasi spherical vesicle in the equatorial plane. These are Eq. 16 in [11], which is the unmodified version of Eq. 2 in the Theory section of this report, and Eq. (5) and Eq. (6) in [6]. We have reproduced these equations here for the convenience of the reader. Eq. 7 and Eq. 8 are reproductions of Eq. (5) and Eq. (6) from [6] respectively.

$$\frac{\kappa}{k_B T} = \frac{S(q)}{\langle |v_q|^2 \rangle} \tag{7}$$

$$S(q) = \sum_{l=q}^{l_{max}} \frac{N_{lq}[P_{pq}(cos\ \pi/2)]^2}{(l+2)(l-1)[l(l+1)+\bar{\sigma}]} \tag{8}$$

where

$$N_{lq} = [(2l+1)/4\pi][(l-q)!/(l+q)!], \bar{\sigma} = \frac{\sigma \langle R \rangle^2}{\kappa}$$

Eq. 9 is a reproduction of Eq. 16 from [11]

$$S_{sh}(n) = \sum_{n=p}^{n=n_{max}} \frac{2n+1}{\pi} \frac{(n-p)!}{(n+p)!} \left(P_n^p(0)\right)^2 \frac{k_B T}{\kappa \lambda_n} \tag{9}$$

where

$$\lambda_n = n^2(n+1)^2 - (2-\bar{\sigma})n(n+1)\ ,\ \bar{\sigma} = \frac{\sigma \langle R \rangle^2}{\kappa}.$$

Note that the adimensional fluctuation spectrum is denoted as $\langle |v_q|^2 \rangle$ in Eq. 7 and as $S_{sh}(n)$ in Eq. 9. Also note that there are small errors in both these formulas: Eq. 8 should have P_{lq} instead of P_{pq}, and $cos\ \pi/2$ could be written more simply as 0. In Eq. 9 it should be $S_{sh}(p)$ instead of $S_{sh}(n)$.

Although these equations claim to describe the same object, and they do indeed look similar, one finds some differences when comparing them. The most significant of these is the factor $\frac{1}{4}$

in N_{lq} in Eq. 8 that is absent in Eq. 9. If we assume that [6] is correct we must conclude that the factor $\frac{1}{4}$ is erroneously missing from [11] to ensure consistency across the papers. We must then also conclude that the factor $\frac{1}{4}$ is missing from Eq. 14 and Eq. B.15 from [11], which are the unmodified versions of Eq. 3 and Eq. 6 in the Theory section of this report, in order to ensure consistency within [11]. That this is required is illustrated in figure 8.

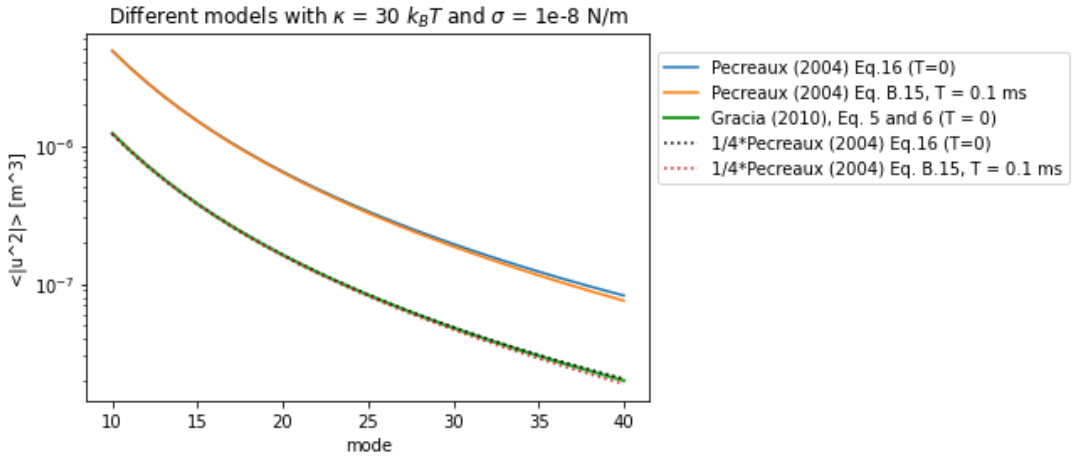

Figure 8: Illustration of a single instance of equations 5 and 6 from Gracia (2010), [6], and of equations 16 and B.15 from Pecreaux (2004), [11], with and without the factor $\frac{1}{4}$.

In this figure it is clear that the addition of the factor $\frac{1}{4}$ causes the graphs to overlap, meaning it causes the models to agree.

The fact that the implementation of VFA that contains the factor $\frac{1}{4}$ in the model for the fluctuation spectrum produces membrane property values that are consistent with the literature, as it is shown to do in section 4.4 and 4.5, further supports the claim that this prefactor is necessary. However, we reiterate that in order to rigorously show the validity of the addition of the factor $\frac{1}{4}$, a derivation should be done.

4.4. Bending rigidity κ obtained using varying shutter speeds and methods of analysis

In order to test the new method and compare it to the old one, we applied all methods to vesicles that were recorded at different exposure times.

A total of six vesicles, labeled as vesicles 5 through 10, were filmed at three different exposure times, 2.5 ms, 5 ms and 10 ms. These were POPC + 0.1% ATTO 655 PE membranes, formed using electroformation in a buffer of 200 mOsm sucrose/glucose + 10 mM Tris. This resulted in 18 videos that were analysed using the old vesicle fluctuation analysis computer program, the old vesicle fluctuation analysis computer program for which the mode selection was done as in the new program, and using the new vesicle fluctuation analysis computer program. The membranes were created and filmed by Lennard van Buren, while the analysis was performed by Abel Hutten. The values for κ and σ thus obtained are shown in table 5 in the appendix. Some videos contained impurities, such as the presence of vesicles other than the target vesicle, which caused the membrane detection software to fail. This was the case for vesicle 6 at 2.5 ms and at 10 ms, and for vesicle 9 at 10 ms. For this reason all data from

vesicles 6 and 9 will be excluded from the following tables and discussion.

All values obtained for κ are shown in figure 9. Some things should be noted from this figure. Firstly, the large deviations in the values produced by the old method of analysis and those produced by the old method with the new mode selection. Secondly, note that a consistent pattern emerges of increasing κ with exposure time when using the old method with the new mode selection, and that this pattern did not hold consistently for the values obtained by the old method. Finally note that when the new method of analysis is applied, the resulting κ's are lower, have a lower variance and do not show a dependence on exposure time. In order to examine specific aspects of this data in more detail, tables 2 through 4 look at statistical moments of interest for subsets of the data that are relevant to the questions we are answering.

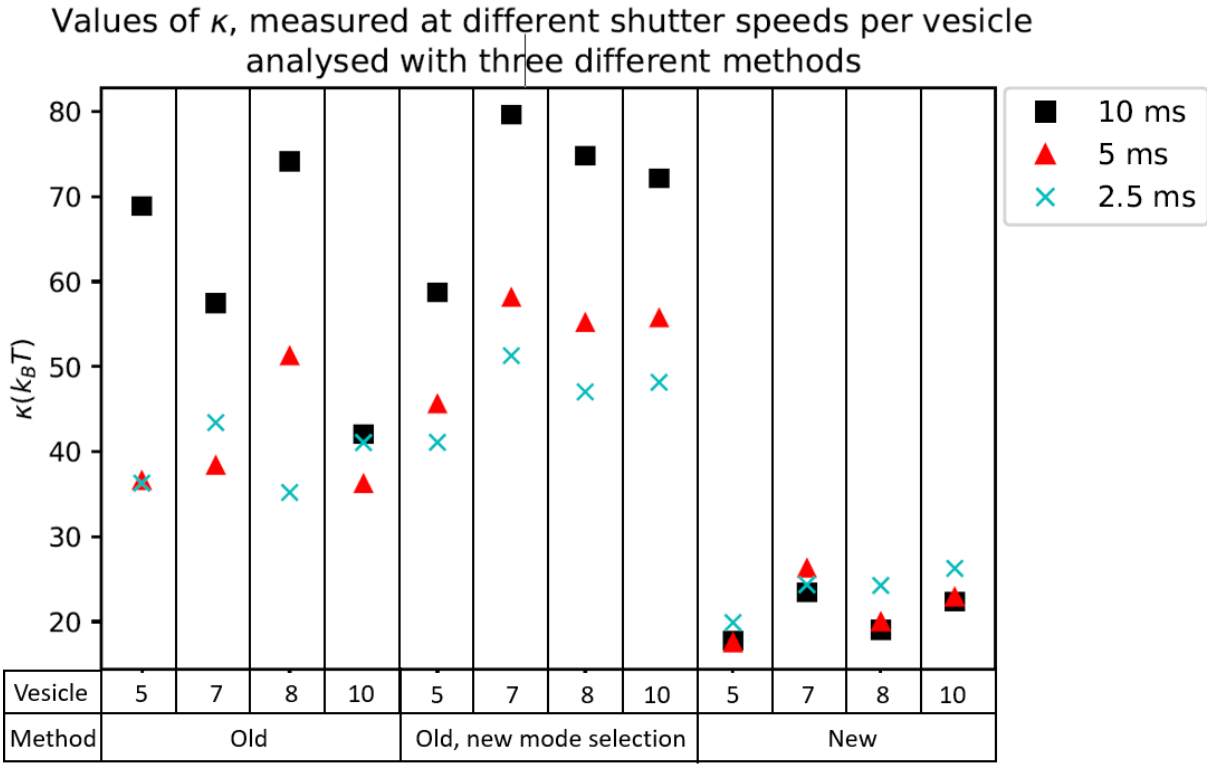

Figure 9: Values of κ for multiple vesicles, measured at different shutter speeds per vesicle, analysed with three different methods. 'Old' denominates the old method, 'Old, new mode selection' denominates the old method with the new mode selection, and 'New' denominates the new method.

For each vesicle and method of analysis, the coefficient of variation (CV) of the values corresponding to the different exposure times was calculated, and these are presented in table 2, together with the mean CV for each method of analysis. The CV is the standard deviation of a data set divided by its mean, which is a dimensionless quantity. We use the CV instead of the variance in order to find the relative variance in the data; since the new method results in a lower mean κ, an equal relative variance would result in a lower absolute variance, making the variance less useful than the CV for comparing the different methods. The CV was calculated in order to examine the effects of the implemented changes on the variability caused by exposure

time in more detail. From this table it can be seen that the relative variance of the obtained values decreases substantially as a result of the changes made in the new program.

Table 2: Coefficient of variation (CV) of κ data, as a function of vesicle and method of analysis. The CV is equal to the standard deviation divided by the mean, and is therefore dimensionless.

Vesicle #	Vesicle Radius (μm)	Old program	Old program, new mode selection	New program
5	5.99	32.4%	15.5%	5.75%
7	8.21	17.4%	19.2%	4.78%
8	7.49	29.9%	19.8%	10.8%
10	8.62	6.38%	17.1%	7.20%
Mean CV		21.5%	17.9%	7.13%

For each exposure time and method of analysis, the average κ over all vesicles has been calculated and is presented in table 3. This allows us to examine the effect of shutter speed for all methods of analysis and to compare the results with the values we expect to see based on the literature.

Table 3: Average κ over the different vesicles, as a function of method of analysis and exposure time, in units of k_BT.

Exposure-time (ms)	Old program	Old program, new mode selection	New program
2.5	38.98	46.88	23.68
5	40.60	53.64	21.65
10	60.62	71.35	20.66

Finally the CV was also calculated as a function of exposure time and method of analysis. The results are presented in table 4. This data allows us to gauge the consistency of each method.

Table 4: Coefficient of variation (CV) of κ data, as a function of exposure time and method of analysis.

Exposure-time (ms)	Old program	Old program, new mode selection	New program
2.5	8.66%	7.87%	9.86%
5	15.3%	8.93%	15.1%
10	20.3%	10.9%	11.2%
Mean CV	14.7%	9.21%	12.1%

Now we will first discuss the effect of the new method of mode selection on the obtained values for κ, by comparing the results of the old method of analysis to that of the old method with the new mode selection. Next we will compare both these methods to the new method, which has the new way of dealing with mode selection as well as a new model for the variance of the fluctuation spectrum that takes into account the exposure time, to discern what effect the implementation of this new model has on the obtained values. The effects that we are most interested in is how the values produced by the different methods compare to the values predicted

by the literature, specifically [10], and how much these values depend on the exposure time.

The effect of changing only the method of mode selection

Both the old method and the old method with new mode selection use the model for the variance in the fluctuation spectrum that assumes zero exposure time. As seen in table 3, this causes the obtained values of κ to generally increase with exposure time on average, as expected. When looking at figure 9, we see that in every single vesicle, the method using the old model with the new mode selection gives values of κ that strictly increase with exposure time, and for which the difference in value between the 2.5 ms and the 5 ms exposure time is smaller than the difference in value between the 5 ms and 10 ms exposure time. For the unaltered old method only 1 out of 4 vesicles, vesicle 8, gives values that strictly increase with exposure time. For the other vesicles this method does not produce the expected increase of κ with exposure time. When looking at table 4 we also see that there is more variance across vesicles when analysing them with the old method compared to the old method with new mode selection, at each exposure time but especially for higher exposure times. Since the vesicles are all produced in the same way, these two findings both support the idea that the old method of mode selection introduces random errors, which can break the pattern of increasing κ with exposure time, and which cause greater variation across measurements on similar vesicles.

This is to be expected, since the old method of dealing with mode selection is more sensitive to the choice of initial mode, meaning the lower boundary for the mode range that is fitted, than the new method, and this choice of initial mode is subjective. The new method of mode selection chooses a range of initial modes where the value of κ changes slowly, and then averages the value of κ over this entire range. Therefore, even if a somewhat different range is selected by the experimenter, the modes that are added or left out will all have similar values to the rest of the range, thus causing only a small change in the mean. The act of averaging itself also reduces the impact of adding or removing small numbers of modes from the selected range.

The choice of upper mode also contributes to the difference in consistency, especially at higher exposure times. Modes with fluctuation lifetime shorter than or similar to the exposure time are effected more strongly by the negative effects of the exposure time. Because higher vibrational modes have lower fluctuation lifetimes (see equation 4), the highest mode used in the fit should be lowered based on the fluctuation lifetime. Since the old method does not explicitly take this into account, it can occur that the upper mode is chosen too high, causing the fit to include modes with inadmissibly high errors caused by the exposure time. This adds randomness to the outcome of the analysis. The new method of mode selection does explicitly limit the highest mode based on exposure time, which explains to a degree why this method produces lower CV values in table 4, and especially why this difference in CV increases with increasing exposure times.

We can conclude that the new method of mode selection improves the consistency of the results obtained from the analysis. In order to explore this improvement further, it would be illuminating to test the analyses on multiple videos taken with the same exposure time, on the same vesicle, since that would eliminate the effect of the variation in κ between the different vesicles, allowing us to see more accurately what the contribution of the mode selection is on the variation in outcomes.

As stated in the theory, the POPC vesicles used are expected to have bending rigidities around 20 k_BT, but varying greatly depending on the exact circumstances. The expected range is between 5 k_BT and 40 k_BT [10]. It is expected that when using the model for the fluctuation spectrum that does not take into account the exposure time, this will result in a κ that is too high, and it is therefore not surprising that modifying the mode selection while not implementing a model that does take the exposure time into account still gives a value that is too high.

The effect of the new method of mode selection in combination with the new model for spectrum variance

Looking at table 3 we see that with the new program, the values for the bending rigidity are right in the expected range, which is an improvement over both the old method and the old method with the new mode selection. From this we can conclude that our new program does indeed produce more accurate values than the old program, and that this change is largely due to the change in the model for the adimensional fluctuation spectrum used for the fit. We also see that the values of κ are lower in this case compared to both the old program and the modified old program, as expected.

When we look at table 2, we see that the CV of the new program is significantly lower than that of both other methods. This is an indication that some dependence on exposure time has been eliminated, since values of κ obtained from the same vesicle at different shutter speeds are now closer together for each vesicle. The pattern of a rising κ with rising exposure time that we see with both other methods has also disappeared, which is another indication that the dependence on shutter speed has been diminished. We now see the opposite trend in table 3; the average value obtained for κ using the new method decreases slightly with exposure time. This is a much smaller dependence on shutter speed however, and when looking at figure 9 we see that this pattern only holds in 2 of the 4 vesicles, suggesting that this trend could be due to the randomness that is still left in the determination of κ. Another fact that instantiates this claim is that the difference in average bending rigidity between the exposure times is of a size similar to the standard deviation of the data. This could be investigated further by measuring a greater number of vesicles at different exposure times, and exploring whether the negative slope of κ with respect to exposure time still remains.

The mean CV of the new method is still non-zero. This is probably due to errors that are not caused by exposure time but by factors such as the membrane detection software, which can introduce errors through contour discretization or incorrectly interpreting the membrane position, or due to slightly different physicochemical conditions between the different videos. It is expected that such errors would cause a bigger CV for vesicles filmed with a higher exposure time, since then the highest mode still used in the fit interval is lower (see table 1), making the fit interval smaller and thereby magnifying the effect of the errors in individual mode amplitudes. When looking at table 4 we do not see this however, since the CV for 5 ms is greater than that of 10 ms. This could easily be due to chance however, since the CV in each table entry is calculated using only 4 data points. It would be interesting for future research to examine a greater number of vesicles at different exposure times to explore this further.

4.5. Membrane tension σ obtained using varying shutter speeds and methods of analysis

The values for σ obtained using varying shutter speeds and methods of analysis are presented in figure 10. As stated the fit is constrained to positive σ values.

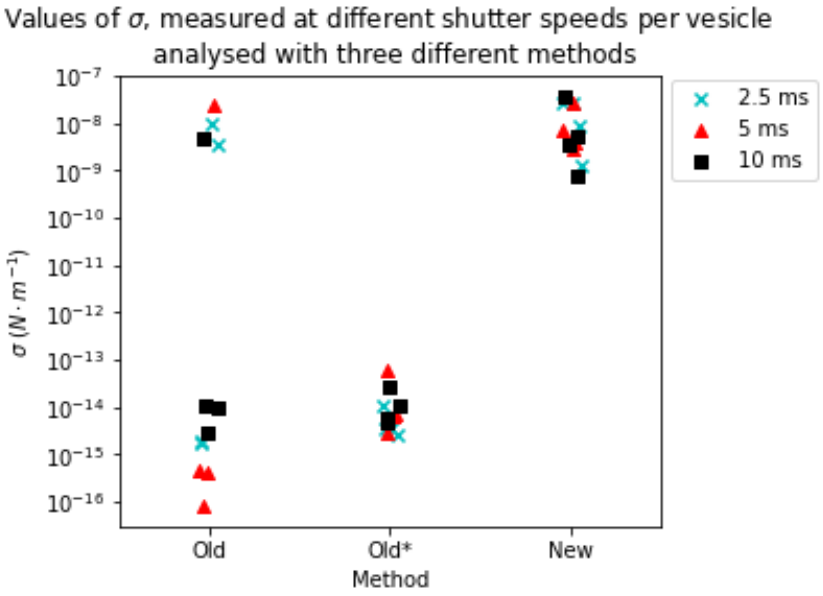

*Figure 10: Values of σ for multiple vesicles, measured at different shutter speeds per vesicle, analysed with three different methods. 'Old' denominates the old method, 'Old *' denominates the old method with the new mode selection, and 'New' denominates the new method.*

As discussed, for both the old method and the old method with new mode selection, we expect the program to overestimate κ and, as a result, underestimate σ. The way in which the zero exposure time model is implemented, as in Eq. 3, there is a division by σ. This makes it impossible for the fit to result in a value of 0 for σ, and σ is then fitted in the $10^{-13} - 10^{-16}$ range, as a result of the details of the structure of the computer and of the software used for the fit. It is interesting to note that none of the data points obtained by the new program fall in the $10^{-13} - 10^{-16}$ range, while all but 4 data points from the other two methods fall into this range. That suggests that σ is no longer underestimated in the new method in order to compensate for an overestimated κ. It is of note that the values of σ generated by the new program vary greatly between exposure times. This is because the theoretical fluctuation spectrum has a very small partial derivative with respect to σ within the fit interval, as seen in figure 6c. Therefore small changes in the observed spectrum have a large impact on the obtained value for σ. Thus this value should only be used as an indication of the order of magnitude, not as an accurate estimation of the true value. In addition, this means that the value we find for κ does not depend strongly on the value we find for σ.

We will not calculate the CV's, nor the average values of σ for each method and shutter speed, because of the way in which the values of σ behave as a function of the method and shutter speed, i.e. by separating into two groups, one in the $10^{-7} - 10^{-9}$ range, and one in the $10^{-13} - 10^{-16}$ range. This makes the values of the CV and the average σ less useful and lends itself better to a more qualitative analysis.

4.6. Validation of analysis by comparison with an independent method

In order to independently check the accuracy of the new method of fluctuation analysis in determining the bending rigidity, we conducted both the new fluctuation analysis and micro pipette aspiration on the same batch of vesicles. A batch of electroformed POPC vesicles was created, and from this batch 13 vesicles were selected for micro pipette aspiration (MPA) measurement. One of these measurements was unsuccessful, resulting in 12 data points. From this batch 3 vesicles were used for fluctuation analysis (VFA), and videos were taken at different exposure times, between 1 ms and 5 ms, for a total of 9 different videos. The MPA measurements, as well as the imaging and subsequent analysis for the VFA measurements were done by Lennard van Buren, who also created the batch of membranes. The results of the micro pipette aspiration measurements and the fluctuation analysis are shown in tables 6 and 7 in the appendix respectively. This data is displayed in figure 11.

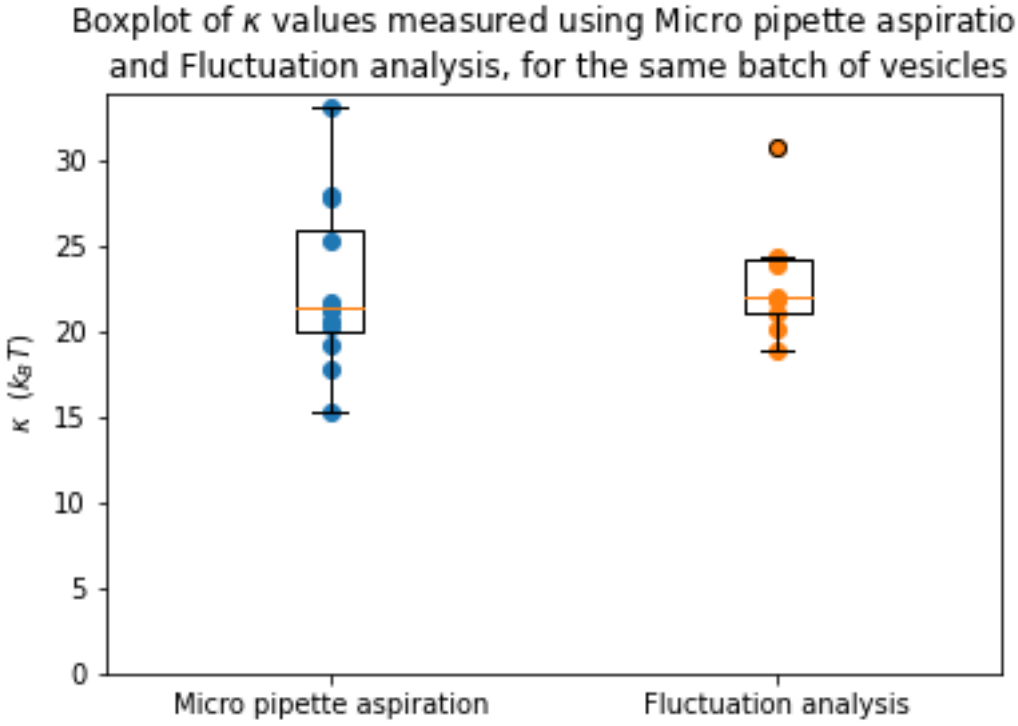

Figure 11: Box plots of κ values from a single batch of vesicles, through both micro pipette aspiration and vesicle fluctuation analysis.

The average values for the bending rigidity of the two data sets are 22.58 k_BT for the MPA data and 22.98 k_BT for the VFA data. Thus, as can be seen in figure 11, both MPA and VFA have given very similar values of κ for this set of vesicles. The means are near identical. The range of values obtained through VFA is smaller, but this is to be expected since the number of vesicles analysed with fluctuation analysis was lower than that analysed with MPA. It is notable that the range of VFA values is completely contained within the range of MPA values. This is strong evidence that the new method of fluctuation data does indeed give accurate values for the bending rigidity. It would be interesting for future research to repeat this experiment with larger sets of measurements and different membrane compositions, in order to give the result more

statistical significance. It would also be interesting to compare MPA and VFA measurements for the same individual vesicles, instead of working with different samples of vesicles from the same batch, as this would remove the randomness introduced by sampling.

5. Conclusion

In this project we have improved the existing vesicle fluctuation analysis procedure, which is used to extract the values of the bending modulus and the tension of a membrane from a video of that membrane. We have shown that measurement with non-zero exposure time has a strong impact on the values obtained from the vesicle fluctuation analysis when the exposure time is not accounted for, by resulting in a bending modulus κ that is too high, which depends on the exposure time of the measurement, and a tension σ that is too low. We have shown that it is necessary to implement an exposure time corrected model for the adimensional fluctuation spectrum in the fit procedure of the analysis. We have improved the existing analysis by implementing a model for the adimensional fluctuation spectrum that takes the exposure time into account. Additionally, we have improved the method of mode selection for the fit procedure, and our improvements have made this process more objective and consistent. This new implementation results in consistent values for κ when measuring a vesicle with different exposure times. Importantly, these values agree with the literature. This allows the experimenter to image with different exposure times while robustly obtaining the correct bending rigidities. We have validated the quality of the improved vesicle fluctuation analysis by comparing its results to independent micro pipette aspiration measurements, and found strong agreement between the results of the two methods. We also conclude that the new method does give an indication of the order of magnitude of the membrane tension but not an accurate value.

References

[1] P.L. Yeagle. *The Membranes of Cells, 3rd Edition*. Academic, Orlando, 1987.

[2] Rumiana Dimova. Recent developments in the field of bending rigidity measurements on membranes. *Advances in Colloid and Interface Science*, 208:225–234, 2014. Special issue in honour of Wolfgang Helfrich.

[3] Derek Marsh. Elastic curvature constants of lipid monolayers and bilayers. *Chemistry and Physics of Lipids*, 144(2):146–159, 2006.

[4] François Liénard. Vesicle fluctuation analysis to measure physical properties of bacterial membranes reconstituted with artificial systems. Biological Soft Matter, Delft University of Technology, Faculty of Bionanoscience, 2020,.

[5] Hammad A. Faizi, Shelli L. Frey, Jan Steinkühler, Rumiana Dimova, and Petia M. Vlahovska. Bending rigidity of charged lipid bilayer membranes. *Soft Matter*, 15:6006–6013, 2019.

[6] R. L. Knorr Reinhard Lipowsky Rumina Dimova R.S. Gracia, N. Bezlyepkina. Effect of cholesterol on the rigidity of saturated and unsaturated membranes: fluctuation and electroformation analysis of giant vesicles. *The European Physical Journal E*, (6):1472–1482, 2010.

[7] Hammad A. Faizi, Cody J. Reeves, Vasil N. Georgiev, Petia M. Vlahovska, and Rumiana Dimova. Fluctuation spectroscopy of giant unilamellar vesicles using confocal and phase contrast microscopy. *Soft Matter*, 16(39):8996–9001, 2020.

[8] Encyclopædia Britannica Inc. Molecular vieuw of the cell membrane. Accessed 08-07-2021. ://www.britannica.com/science/cell-membrane.

[9] E.M. Lifshitz L.D. Landau. *Theory of Elasticity. Vol. 7 (3rd ed.)*. Butterworth-Heinemann, 1986.

[10] G. Khelashvili M. Doktorova, D. Harries. Determination of bending rigidity and tilt modulus of lipid membranes from real-space fluctuation analysis of molecular dynamics simulations. *Phys. Chem. Chem. Phys.*, (9):16806–16818, 2017.

[11] J. Prost J.-F. Joanny P. Bassereaux J. Pecreaux, H.-G. Dobereiner. Refined contour analysis of giant unilamellar vesicles. *The European Physical Journal E*, (13):277–290, 15-1-2004.

[12] A. Courant D. Hilbert. *Methods of Mathematical Physics, Volume 1*. Interscience Publischer, Inc, New York, 1953.

[13] W Helfrich. Elastic properties of lipid bilayers: Theory and possible experiments. *Zeitschrift für Naturforschung C*, 28(11-12):693–703, 1973.

[14] *A dictionary of physics*. Oxford University Press, 2005.

[15] Scott T. Milner and S. A. Safran. Dynamical fluctuations of droplet microemulsions and vesicles. *Physical Review A*, 36(9):4371–4379, 1987.

[16] Don S. Lemons and Anthony Gythiel. Paul langevin's 1908 paper "on the theory of brownian motion" ["sur la théorie du mouvement brownien," c. r. acad. sci. (paris) 146, 530–533 (1908)]. *American Journal of Physics*, 65(11):1079–1081, 1997.

[17] scipy.optimize.least_squares. Fit procedure documentation. Accessed 8/7/2021. `ttps://docs.scipy.org/doc/scipy/reference/generated/scipy.optimize.least_squares.`html#scipy.optimize.least_squares.

[18] Miglena I. Angelova and Dimiter S. Dimitrov. Liposome electroformation. *Faraday Discuss. Chem. Soc.*, 81:303–311, 1986.

[19] Andreas Weinberger, Feng-Ching Tsai, Gijsje H. Koenderink, Thais F. Schmidt, Rosângela Itri, Wolfgang Meier, Tatiana Schmatko, André Schröder, and Carlos Marques. Gel-assisted formation of giant unilamellar vesicles. *Biophysical Journal*, 105(1):154–164, 2013.

[20] J. R. Henriksen and J. H. Ipsen. Measurement of membrane elasticity by micro-pipette aspiration. *The European Physical Journal E*, 14(2):149–167, 2004.

[21] Timon Idema. Personal correspondence , 2021.

Appendix

Table 5: Measured values of κ and σ for individual electroformed vesicles filmed at different shutter speeds, analysed with three different methods. Entries are of the form $[\kappa\,(k_BT)\,,\ \sigma\,(N\cdot m^{-1})]$.

Vesicle #	Exposure-time (ms)	Old program	Old program, new mode selection	New program
5	2.5	36.28 , 1.83 $\cdot 10^{-15}$	41.09 , 3.60 $\cdot 10^{-15}$	19.88 , 8.30 $\cdot 10^{-9}$
	5	36.59 , 4.53 $\cdot 10^{-16}$	45.57 , 6.66 $\cdot 10^{-15}$	17.50 , 4.00 $\cdot 10^{-9}$
	10	68.85 , 9.30 $\cdot 10^{-15}$	58.76 , 4.92 $\cdot 10^{-15}$	17.80 , 3.50 $\cdot 10^{-9}$
6	2.5	Membrane detection fails		
	5	82.86 , 3.36 $\cdot 10^{-8}$	78.62 , 9.39 $\cdot 10^{-8}$	27.45 , 1.03$\cdot 10^{-7}$
	10	Membrane detection fails		
7	2.5	43.40 , 3.59 $\cdot 10^{-9}$	51.28 , 2.48 $\cdot 10^{-15}$	24.34 , 2.66 $\cdot 10^{-8}$
	5	38.36 , 8.31 $\cdot 10^{-17}$	58.11 , 2.88 $\cdot 10^{-15}$	26.25 , 7.29 $\cdot 10^{-9}$
	10	57.47 , 2.77 $\cdot 10^{-15}$	79.65 , 2.72 $\cdot 10^{-14}$	23.42 , 5.35 $\cdot 10^{-9}$
8	2.5	35.18 , 1.87 $\cdot 10^{-15}$	47.02 , 1.05 $\cdot 10^{-14}$	24.24 , 2.48 $\cdot 10^{-8}$
	5	51.24 , 4.42 $\cdot 10^{-16}$	55.16 , 7.54 $\cdot 10^{-15}$	19.96 , 2.91 $\cdot 10^{-9}$
	10	74.13 , 1.07 $\cdot 10^{-14}$	74.80 , 1.06 $\cdot 10^{-14}$	19.03 , 3.35 $\cdot 10^{-8}$
9	2.5	39.27 , 1.34 $\cdot 10^{-8}$	49.62 , 1.26 $\cdot 10^{-14}$	25.86 , 1.45 $\cdot 10^{-9}$
	5	39.72 , 2.42 $\cdot 10^{-15}$	62.91 , 9.90 $\cdot 10^{-15}$	25.78 , 3.26 $\cdot 10^{-8}$
	10	Membrane detection fails		
10	2.5	41.05 , 9.90 $\cdot 10^{-9}$	48.14 , 3.54 $\cdot 10^{-15}$	26.25 , 1.34 $\cdot 10^{-9}$
	5	36.21 , 2.25 $\cdot 10^{-8}$	55.70 , 6.29 $\cdot 10^{-14}$	22.89 , 2.74 $\cdot 10^{-8}$
	10	42.01 , 4.85 $\cdot 10^{-9}$	72.18 , 6.09 $\cdot 10^{-15}$	22.38 , 7.19 $\cdot 10^{-10}$

Table 6: Micro pipette aspiration

Vesicle #	$\kappa\,(k_BT)$
1	21.2
2	33
3	25.2
4	20.2
5	17.8
6	20.5
7	FAIL
8	21.7
9	27.9
10	27.7
11	15.2
12	21.4
13	19.1

Table 7: Fluctuation analysis values of κ for electroformed POPC vesicles used in the comparison with micro pipette aspiration data (table 6.

Vesicle #	Exposure time (ms)	$\kappa\ (k_BT)$
1	1	30.7
1	1	21.2
1	5	23.9
1	5	24.3
1	5	24.1
2	2	20.1
2	2	18.9
3	3	21.8
3	3	21.9